Research Article

Achieving Adjustable Wettability in Graphene-Based Films Using a Facile Technique

Liqiu Zheng[1*] **and Yonglin Zhao**[2]

[1]*Department of Chemistry and Forensic Sciences, Albany State University, Albany, USA*

[2]*School of Science, Nantong University, Nantong, China*

*Corresponding author: Liqiu Zheng, Department of Chemistry and Forensic Sciences, Albany State University, Albany, USA, Tel: 0012294207052; E-mail: Liqiu.Zheng@asurams.edu

Citation: Zheng L, Zhao Y (2024) Achieving Adjustable Wettability in Graphene-Based Films Using a Facile Technique. Journal of Nanotechnology and Nanobiotechnology, 1(1):101.

Abstract

A facile, safe and low cost thermal approach was developed to regulate wettability of graphene-based surfaces from superhydrophilicity to superhydrophobicity, which promises mass production on surface technology in various industrial applications. The long-lasting stable superhydrophobicity was attained by hydrogenating graphene with chem-absorbed functional groups. Meanwhile, the approach paves the way for producing fully hydrogenated graphene, which is an entirely novel material called graphene.

Keywords: Wettability; Superhydrophilicity; Superhydrophobocity; Hydrogenation; Graphane

Introduction

Graphene, one of the thinnest materials known [1], is a single-atom-thick sheet comprised of sp2-hybridized carbon atoms, arranged in a hexagonal lattice. Uanks to its unique single-atom structure, graphene is a complete surface material in which virtually all atoms are exposed to the environment, which provides a fertile playground for researchers to manipulate its surface properties, for instance, tailor its wettability from wetting to non-wetting, in both theoretical and experimental fields. However, extensive research has been mainly focused on photoelectric performance of graphene, because of its other extraordinary features which find numerous novel device applications. For instance, its excellent electronic transport performance is widely utilized in electronics fields [2]; robustness and light weight in micromechanical resonators [3]; high conductivity in electrical batteries [4]; high surface-to-volume ratio, atomic thinness in field emitters [5] and optical transparency in transparent membranes for electron microscopy. In contrast, far less attention has been devoted to the properties of graphene surfaces, although controllable manipulation of wetting behaviors on graphene surface promises equally significant technological applications in various fields such as micro-fluidics, water harvesting, anti-fouling, and anti-corrosion [6]. As far as wettability is concerned, the more striking feature of conformal graphene coatings is wetting transparency, which could exist when mono-layer graphene is deposited on the appropriate substrates (such as copper, gold or silicon) [7-9], which refers to the fact that Van der Waals forces between water and substrate are able to be seen through graphene layer, due to the extreme thinness of graphene. Ue wetting transparency of graphene enables even wider applications in which electronic and wetting properties can be independently controlled, leading to the design of multifunctional smart surfaces.

Currently, some attempts have been prompted to control wettability of graphene films. Surface properties are governed by surface physical architecture and chemical composition, which leads to two directions: one is to engineer morphological patterns on surfaces; the other is to alter surface chemical composition. Laser interference and lithographic techniques are mostly taken to fabricate patterned roughness on graphene to realize desired wettability. Uese techniques require costly sophisticated equipment and fussy manipulation [10,11]. Consequently, altering chemical composition through functionalizing surface predominates in tuning wettability of graphene. For example, Rafiee et al. [12] developed a technique to regulate wettability of graphene films from super hydrophilicity to super hydrophobicity by sonicating graphene in water and acetone solutions with di9erent concentration. Although a controllable contact angle (CA) changes from 0° to 160°, physic-absorbed functional groups by sonication are not stably graled onto graphene films which results in a quick loss of super hydrophobicity. Meanwhile, long time sonication of graphene films produces lots of undesired defects. Fluorinated graphene [13,14] is another e9ective but cumbersome approach which produces very limited yield and o9ers no avenue for scale up. Additionally, in the process XeF_2 and HF are involved which pose serious safety issues. Uerefore, it is imperative to develop a facile, inexpensive, safe and scalable approach to achieve tunable wettability of graphene films for practical applications.

In this contribution, for the first time we reported a facile method to tune the wettability of graphene-based films from super hydrophilicity to super hydrophobicity. Uis low cost, safe approach is of vital technological importance because of its scalability which would promise various industrial applications, ice mitigation, advanced multifunctional coatings and composites [15,16]. More importantly, the approach holds great potential for transforming graphene into an entirely novel material called graphane when fully hydrogenated, which would find even wider applications in di9erent fields.

Materials and Methods

A few layers of graphene powder (Angstrom Materials LLC, 1.5 g, carbon content 97%) was sonicated in 120 mL of a 3:1 mixture of H_2SO_4 (18 M) and HNO_3 (17 M) at 40°C for 4 hours. Ue dispersion

was allowed to stand at room temperature for 3 days. Aler repeatedly washed with water (total 4 L), by centrifugation and decantation, the oxidized graphene was filtered through a 0.2 µ Polytetrafluoroethylene (PTFE) membrane, with a final ethanol wash. Ue product was allowed to dry under vacuum overnight. Ue dried product was dissolved in 50 mL of Dimethylformamide (DMF) (Fisher Chemical ≥ 99.8%). Ue total amount of as-produced graphene oxide was divided into 4 portions with equal amount for 4 di9erent batches of samples. All portions were air-brushed onto quartz slides and then placed on a heating plate at 150°C in order to remove the DMF solvent from coating. Instantly, the first batch, graphene oxide, was obtained. Ue other 3 batches was ready for further treatment. Two batches of quartz slides with graphene coating were put into a tubing furnace under hydrogen (H_2) flow with 20 ml/min. Aler 30 mins of reduction at 350°C, one batch was taken out for various characterizations. Uen aler another 30 mins, the second batch was taken out. Next, a pre-prepared Ni (8%wt)/Al_2O_3 catalyst in a graphite boat was placed upstream of the H_2 flow (Note: Preparation for catalyst: Ue nickel nitrate hydrate (Ni(NO_3)$_2$·6H_2O) solution with Al_2O_3 powder (BET 270 m^2/g) was ultra-sonicated and dried at 110°C, ground to a fine powder, and then calcined at 500°C for 2 hours). Ue catalyst-containing graphite boat and the last batch of graphene coating quartz slides were kept 5 inches apart. Ue temperature was raised to 800°C and maintained for 200 mins. Ue final step was to naturally cool down the furnace to room temperature under H2 flow. Wettability was evaluated by water contact angle goniometry. Morphological structure information was revealed by scanning electron microscopy (SEM) (JEOL JSM-7000F), transmission electron microscopy (TEM) (JEOL JEM-2100F) and atomic force microscopy (AFM) (Bruker Nano). Chemical composition was scrutinized by Fourier transform infrared spectroscopy (FTIR) (Agilent Cary 630) and Raman Spectroscopy (Horiba Jobin Yvon Lab Ram 800).
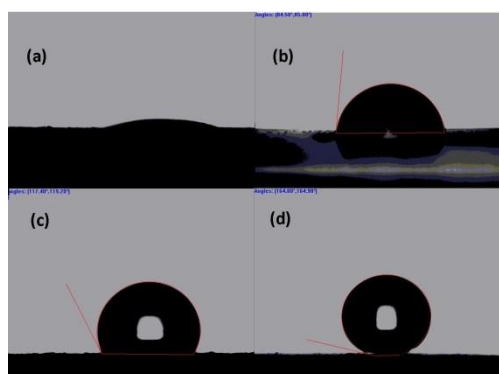
Results and Discussion

Figure 1: Wettability properties of di9erently treated graphene-based films. (a) As-produced graphene-based film; (b) graphene-based film with 30-min reduction; (c) graphene-based film with 60-min reduction; (d) Hydrogenated graphene-based film.

Wettability of samples was characterized by CA measurements. CA is a conventionally measured angle between a tangential line along a liquid–vapor interface and a base line where the liquid meets a solid surface. It quantifies wettability of a solid surface. If CA >90° the solid surfaces are categorized as hydrophobicity. If CA<90°, the surfaces are hydrophilicity. For the extreme cases, if CA>150° surfaces are called a super hydrophobicity and if CA<10°, surfaces are a super hydrophilicity [17]. Vastly di9erent wettability was demonstrated by graphene-based coatings in Figure 1. Figure 1a displays the super hydrophilicity of as-produced graphene-based surface because CA is much smaller than 10°. A water droplet deposited onto the surface instantly spread out and formed a water film, revealing an abundantly hydrophilic nature of as-produced graphene-based (graphene oxide) plane. Figure 1b depicts slightly reduced graphene-based surfaces with the CA of 84° ± 2° aler 30 mins reduction, an obvious increase in CA observed. Although the surface is still in the hydrophilic range, the hydrophilic nature was greatly weakened by 30 mins reduction treatment. Aler further treatment by extending the reduction time to 60 mins, the water CA increased to 117° ± 2° as seen in Figure 1c which falls into the hydrophobic category. Ue results are consistent with previous reports [18]. Ue inherent hydrophobic nature of graphene sheet dominated aler the thermal removal of hydrophilic functional groups, which altered the surface to be hydrophobic. But there was no noticeable increase in CA observed on those graphene films when the reducing time extends even longer than 200 mins (for instance, the graphene films were reduced at 800°C without catalyst. Not shown here). In contrast, hydrogenation caused a dramatic change in wettability on the surface because CA increased to164° ± 2° as revealed in Figure 1d, which is much larger than 150°. Additionally, the contact angle of 164° ± 2° was measured aler the samples were exposed to ambient conditions for 2 months. Super hydrophobicity was achieved aler hydrogenation. Ni (8%wt)/Al_2O_3 catalyst breaks down the hydrogen-hydrogen molecule bond into atomic hydrogen. Uese atomic radicals combine with dangling carbon bonds which are lel behind by the elimination of other groups forming C-H bonds. Ue chemically absorbed functional groups -CH_2 or -CH_3 onto graphene sheet induce a long lasting super hydrophobicity. Tunable wettability from super hydrophilicity to super hydrophobicity was achieved by this facile, low cost, and safe approach which is ready for mass production.

As aforementioned, surface morphological roughness and chemical composition play parts in surface properties. In order to examine surface structure, samples were thoroughly scrutinized by SEM, AFM and TEM. As an ideal two dimensional material, graphene has even higher specific surface area than its allotrope carbon nanotubes [19]. Its lateral sheet can extend up to tens of micrometers as revealed by all images in Figure 2. Figure 2a discloses that micron-sized graphene oxide sheets have a flaky texture, reflecting their layered microstructure. Air-brushed graphene films created inherent roughness which stems from random arrangement of graphene sheets. Figures 2b and 2c portray morphology of graphene-based sheets aler reduction 30 minutes and 60 minutes, respectively. Figure 2d depicts the surface structure of the hydrogenated graphene. All SEM images suggest that the high aspect ratio and large nominal surface areas of flaky graphene were not altered by reduction/hydrogenation treatments. All the graphene-based films demonstrate a structure of individual flakes with highly wrinkled, folded and buckled edges, which generated di9erent scale roughness that can be down to nano-size. Ue average surface roughness established hierarchical structures on the films.
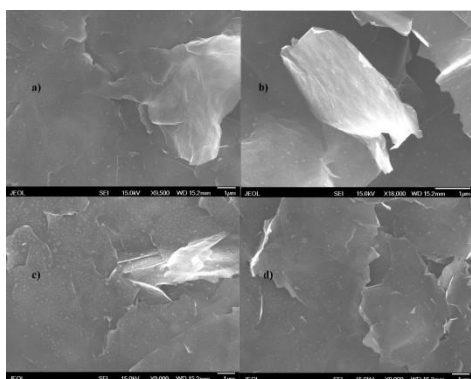
Figure 2: Scanning electron microscopy (SEM) images (a) as-produced graphene-based film; (b) graphene-based film with 30-min reduction (b) graphene-based film with 60-min reduction; c) hydrogenated graphene-based film.
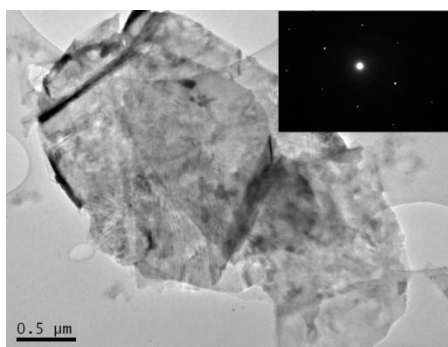

Figure 3: Transmission electron microscopy (TEM) image for hydrogenated graphene-based film; Insert is reciprocal lattice peaks obtained by 2D Fourier transform based on TEM image for hydrogenated graphene-based film.

TEM in Figure 3 further confirms that the flaky transparent feature of graphene-based film was maintained even aler hydrogenation. Particularly, it is worth mentioning that hydrogenation did not change the hexagonal arrangement of carbon atoms as characterized in the insert of Figure 3, in which reciprocal lattice peaks were obtained by 2D Fourier transform based on TEM image of the hydrogenated graphene-based film.
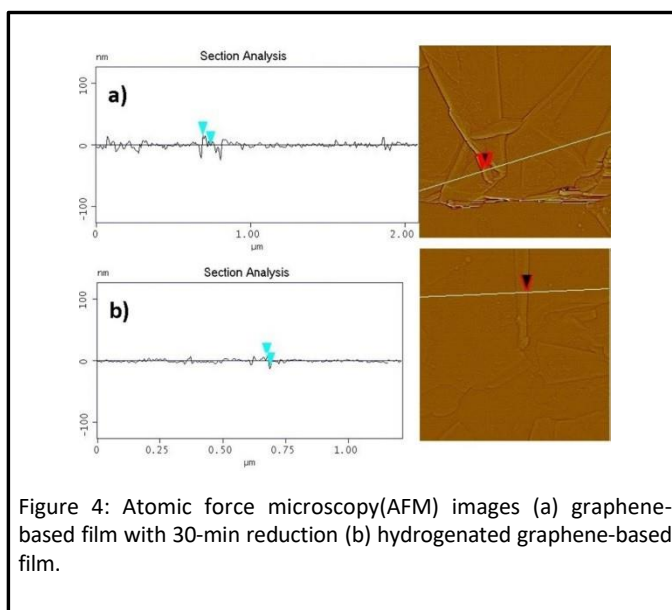

Figure 4: Atomic force microscopy(AFM) images (a) graphene-based film with 30-min reduction (b) hydrogenated graphene-based film.

AFM images further corroborate the morphological analysis. As revealed by SEM images, AFM images in Figure 4 substantiate similar graphene flakes with randomly stacked and crumpled surface structure. Ue roughness on surfaces is up to ten nanometers on individual graphene sheet, consistent with SEM results. Figure 4a demonstrates morphology of graphene-based film aler 30 minutes reduction and Figure 4b presents the surface structure of graphene-based film aler hydrogenation. Ue comparison of both AFM images shows that reduction and hydrogenation procedures did not result in any noticeable changes in the structural morphology. It is important to note that increased time reduction does not make any di9erence in morphology when comparing SEM of graphene-based film aler 60 minutes reduction in Figure 2b with AFM of graphene-based film aler 30 minutes reduction in Figure 4a.

In spite of similar surface morphology, samples display strikingly di9erent wetting behaviors. To clarify the underlying reason behind this phenomenon, FTIR was adopted to probe surface chemical composition. Figure 5a depicts the transmittance spectra of graphene oxide films in which characteristic peaks of graphene oxide correspond to: alkoxy C-O (1116 cm^{-1}); epoxy C-O (1228 cm^{-1}); stretching single bond carboxy C-O (1414 cm^{-1}); stretching double bond carboxy C=O (1735 cm^{-1}). While a broad peak is supposed to appear at 3442 cm^{-1} which is ascribed to the water O-H stretching vibration. Notably, this peak blue-shiled above 3500 cm^{-1} in graphene oxide as seen in Figure 5a on the grounds that the stretching bond became very rigid aler the loss of electrons to strong acid which is in good agreement with other reported results in the literatures [20]. Ue presence of oxygen functionalities on the basal plane carbon atoms rendered the as-produced graphene-based film a super hydrophilic nature, which explains why water droplets spread into a thin film instantly when deposited on graphene oxide films. It is worth pointing out that the graphene oxide undergoes acid treatment which considerably increased wettability of samples since it brought additional polar OH groups and oxygen functional groups like carboxyl and epoxyl onto the surface of grapheme [21]. On the other hand, acid treatment created defects in graphene which opens possibilities for functional groups addition and thus varying properties around defect sites.
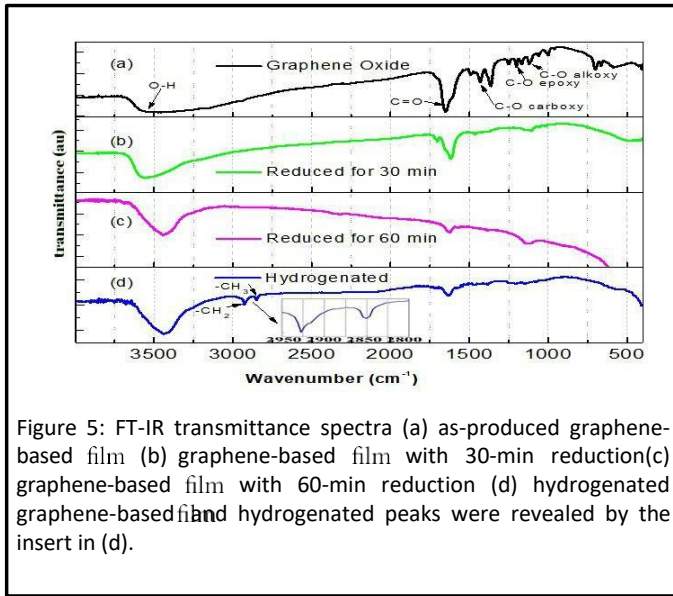
Figure 5: FT-IR transmittance spectra (a) as-produced graphene-based film (b) graphene-based film with 30-min reduction(c) graphene-based film with 60-min reduction (d) hydrogenated graphene-based film and hydrogenated peaks were revealed by the insert in (d).

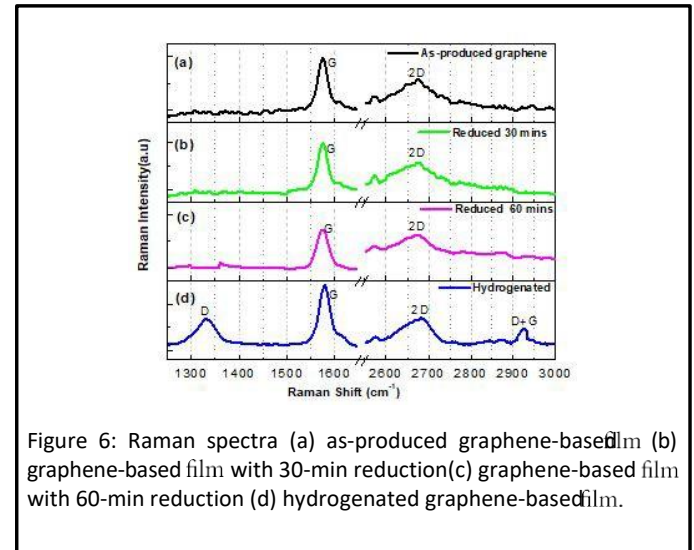and inexpensive approach which holds promise for mass production and creating novel graphane.

Figure 6: Raman spectra (a) as-produced graphene-based film (b) graphene-based film with 30-min reduction(c) graphene-based film with 60-min reduction (d) hydrogenated graphene-based film.

As observed in Figure 5b, after 30 min reduction, some oxygen functional groups like carboxy C=O (1735 cm^{-1}) dramatically decreased while others like carboxy C-O (1414 cm^{-1}) were completely eliminated which accounts for the increase in CA from less than 10° to 84° ± 2°. It suggests that the hydrophilic functional groups on the surface of graphene films were partially removed. In addition, 30-min reduction did not soften the broad peak of O-H stretching mode and no red shift was observed because it is still above 3500 cm^{-1} as indicated in Figure 5b. Further reduction of 60 mins resulted in the riddance of virtually all oxygen functional groups as shown by Figure 5c. Accordingly, CA increased to 117°±2°. The elimination of carboxyl and hydroxyl groups from basal plane of graphene allowed an intrinsically hydrophobic nature of graphene unearthed which was also reflected by a strong tendency of graphene powder to agglomerate in aqueous solvents after 60 mins reduction. Although there was a recognizable difference in CA between 30 mins and 60 mins reduction treatments, CA remained 117° ± 2° even when reduction time extended longer than 200 minutes. Therefore 164° ± 2° CA on hydrogenated graphene-based film did not result from the longer treatment time (200 mins) of hydrogenation but the presence of catalyst Ni (8%wt)/Al$_2$O$_3$, which made atomic hydrogen available by breaking down hydrogen-hydrogen molecule bonds and accomplishes the decoration of functional groups -CH$_2$ or -CH$_3$ onto graphene sheet as displayed Figure 5d. Particularly, the insert in Figure 5d clearly discloses that additional peaks 2926 cm^{-1} and 2853 cm^{-1} are the stretching modes of H bonded to olefinic carbon and the bending modes of H bonded to aromatic carbon, respectively. The introduction of hydrogenated groups lowers surface energy of graphene sheet, leading to a stable super hydrophobicity, which explains why CA reached 164° ± 2° after hydrogenation due to the fact that grafted hydrocarbon groups enhance hydrophobicity of the graphene surface. Remarkably, the broad water peak of O-H stretching mode, after gaining electrons, softened down to 3442 cm^{-1} as shown in Figures 5c and 5d. The adsorption of oxygen functionalities or hydrogen groups on graphene can be used to tailor wettability properties of graphene-based films, as already suggested for the modified wetting graphene films which are sonicated in acetone [12]. Tunable wettability from super hydrophilicity to super hydrophobicity was achieved with a facile

Raman spectroscopy decisively substantiates the FTIR results. As revealed in all images in Figure 6, there are two intense characteristic peaks of graphene, which are G band at 1580 cm^{-1} and 2D band at 2700 cm^{-1}. The G band is due to the in-plane vibrational (E2g) mode, while the 2D band results from the two phonon inter-valley double resonance scattering [22,23]. It is worth pointing out that the red-shift of the 2D band to below 2700 cm^{-1} at around 2685 cm^{-1} is caused by multilayer of graphene for Raman characterization. The 2D peak of one-layer graphene would show up at 2700 cm^{-1}. The number of layer of graphene causes red-shift because the 2D band acts as the fingerprint in distinguishing one-layer or multilayer. Compare with Figures 6a-6c, besides G and 2D bands, there are two additional peaks which are assigned to D (1340 cm^{-1}) and D+G (2920 cm^{-1}) bands as shown in Figure 6d. The observation of D and D+G peaks amply illuminates that defects were introduced onto the graphene lattice by the hydrogenation treatment, which were the newly formed C-H sp3 bonds and the breaking of the translational symmetry of C=C sp2 bonds [24]. CA for a smooth surface can be expressed in the form of Young's equation [25,26]:

$$\cos\theta = (\gamma_{sv} - \gamma_{sl})/\gamma \quad (1)$$

In equation (1), surface energies of solid-liquid, solid-vapor and liquid-vapor interfaces are denoted by γsv, γsl, γ, respectively. To describe textured surfaces there are two models known as "Wenzel" [27] in equation (2) and "Cassie-Baxter" in equation (3) [28].

$$\cos\theta^* = r\cos\theta \quad (2)$$

$$\cos\theta^* = f_A\cos\theta - f_B\cos\theta \quad (3)$$

In equation (2) Wenzel model, θ* is the effective CA on the textured surface; r is the roughness ratio; and θ is the Young CA on a flat solid surface. In equation (3) Cassie-Baxter model, θ is the effective CA; fA and fB are fractions of surface area of components A and B; θ$_A$ and θ$_B$ are the Young CAs on flat surfaces of A and B, respectively. The difference between two models is whether the liquid drop retains intimate contact with a solid surface at all points or whether the liquid bridges across surface protrusions, thus, resulting in a drop sitting on a

composite solid and vapor surface, suggesting that the textured surface must have the capability of entrapping air pockets. Ue former is a Wenzel model which applies to hydrophilicity or mild hydrophobicity. Ue latter is a Cassie-Baxter model which applies to strong or super hydrophobicity. Due to high surface energy of surfaces, the strong adhesion between graphene surfaces and water droplet compels an intimate contact which does not allow air being entrapped between those textures. Hence, equation (2) Wenzel model explains CAs from smaller than 10° in Figure 1a to 117° ± 2° in Figure 1c. Ue actual CA is mainly determined by the Young CA on the flat surface and amplified by the roughness ratio r. It suggests that graphene oxide surfaces with abundant hydrophilic groups, along with 30 mins reduced graphene-based surfaces, still remains hydrophilic even with certain roughness. Aler 60 mins reduction, an intrinsic hydrophobicity is brought to light by the removal of nearly all hydrophilic groups. Ue CA remains the same aler the complete exposure of intrinsic hydrophobicity of graphene-based film by even longer-time reduction. CA can be further enhanced by lowering surface energy when altering surface chemical composition [29]. Reportedly, the introduction of functional groups like –CF3, –CH3 and –CH2 could effectively lower surface energy, realizing super hydrophobicity [30]. For super hydrophobicity, Cassie-Baxter equation (3) is adopted to describe strong or super hydrophobicity, in which there are three requirements optimizing surface conditions and thus maximizing CA. Ue first one is that the surface must have an ability to capture air pockets in its architectures. When the surface is capable of entrapping air bubbles, fractions of surface area of components A and B will be a solid portion and an air portion. Ue CA B in air is 180o (then $= -1$) and $= 1 -$ which leads to the simplification of equation (3) as:

$$^* = -(1 -)\ (4)$$

Uen aler further simplifying, equation (4) becomes more compact as:

$$^* = (+ 1) - 1\ (5)$$

In order to obtain a maximal CA, the larger portion of water sitting on the air bubble leads to the higher effective CA suggesting the second optimal condition is that a smaller f_A is required. Ue third one is that the Young CA $_A$ on the solid portion is as large as possible which could maximize the effective CA. In the hydrogenated graphene-based film's case, the topology of graphene flakes, together with weak adhesion induced by low surface energy, allows air to be entrapped within wrinkles or folds underneath a water drop which satisfies the first optimal condition. Ue second condition for maximal CA is that the fraction of solid portion f_A should be minimized, which implies the larger portion of a water droplet would sit on air which allows for 180°. As one of the thinnest known materials, the folded/wrinkled/buckled edges of graphene flakes protrude on surfaces supporting water droplets which drastically decrease the contact area of a droplet with the nano-protrusions. In other words, a smaller area fraction, fA, is realized by the morphologically thin character of graphene, which meets the second optimal requirement. Ue third optimal condition requires a larger $_A$, the Young CA on a flat surface, which can be fulfilled merely by lowering the surface energy. Acid treatment opens possibilities for functional groups addition which enhances the reactivity for functionalizing them with low surface energy groups. As a result, with catalyst breaking H2 molecule bond into atomic hydrogen, functional groups -CH2 or -CH3 are formed and then chemically absorbed onto the graphene sheet, leading to a long lasting stable super hydrophobicity. It implies that the decoration of -CH₂ or -CH₃ groups onto graphene films lowers the surface energy which yields a larger CA and thus achieves the third optimizing condition.

Uerefore, apart from the geometrical microstructure, the chemical composition of the surface also plays an important role in wettability properties of graphene-based films. Ue random stacking of graphene sheets introduces inherent roughness, along with modulating surface chemical composition, which suffices to regulate wettability from super hydrophilicity to super hydrophobicity.

Conclusion

In summary, the thermal reduction of graphene-based films is accompanied by the elimination of epoxy, carbonyl/carboxyl groups and the introduction of hydrocarbon groups, which can regulate wettability of graphene-based surfaces from super hydrophilicity to super hydrophobicity. By varying the reduction time, the amount of those hydrophilic groups plays a part in tailoring wettability of the surfaces. A facile and low cost approach to hydrogenate graphene with Ni (8%wt)/Al2O3 catalyst, readily realizes super hydrophobicity which meantime promises for scaled-up production. If all of the oxygen groups are removed, and the sample becomes fully hydrogenated, an even higher CA can be achieved. More importantly, a completely novel material named graphane is potentially created by fully hydrogenating graphene. Uanks to its low mass and large surface area, along with other exceptional properties, graphene-based film with tunable wettability could be used as a multifunctional coating material for various applications in solar panel, aerospace, aviation, and even anti-icing fields.

References

1. Si Y, Samulski ET (2008) Synthesis of water soluble graphene. Nano Lett 8: 1679-1682.

2. Jana S, Singh JK, Kwak SK (2009) Vapor-liquid critical and interfacial properties of square-well fluids in slit pores. J Chem Phys 130: 214707.

3. Chen C, Rosenblatt S, Bolotin KI, Kalb W, Kim P, et al. (2009) Performance of monolayer graphene nanomechanical resonators with electrical readout. Nat Nanotechnol 4: 861-868.

4. Casolo S, Løvvik OM, Martinazzo R, Tantardini GF (2009) Understanding adsorption of hydrogen atoms on grapheme. J Chem Phys 130: 054704-054714.

5. Eda G, Unalan HE, Rupesinghe N, Amaratunga AGG, Chhowalla M (2008) Field emission from graphene based composite thin films. Appl Phys Lett 93: 233502-233505.

6. Hu HW, Allen CK, Li JH, Kong YY, Wang XW, et al. (2014) Multifunctional organically modified graphene with super-hydrophobicity. Nano Res 7: 418-433.

7. Kim GT, Gim SJ, Cho SM, Koratka N, Oh IK (2014) Wetting-transparent graphene films for hydrophobic water-harvesting surfaces. Adv Mater 26: 5166-5172.

8. Mugele F (2012) Wetting: Unobtrusive graphene coatings. Nat Mater 11: 182-183.

9. Rafiee J, Mi X, Gullapalli H, Uomas AV, Yavari F, et al. (2012) Wetting transparency of grapheme. Nat Mater 11: 217-222.

10. Huang YY, Chen XD, Zhang MQ (2014) Reversible surface wettability conversion of graphene films: optically controlled mechanism. J Mater Sci 49: 3025-3033.

11. Naghdi S, Jaleh B, Shahbazi N (2016) Reversible wettability conversion of electrodeposited graphene oxide or titania nanocomposite coating: Investigation of surface structures. Appl Surf Sci 368: 409-416.

12. Rafiee J, Rafiee MA, Yu ZZ, Koratkar N (2010) Super hydrophobic to superhydrophilic wetting control in graphene films. Adv Mater 22: 2151-2154.

13. Galande C, Gao W, Mathkar A, Dattelbaum AA, Narayanan TN, et al. (2014) Science and engineering of graphene Oxide. Part Part Syst Charact 31: 619-638.

14. Jayaramulu K, Datta KKR, Rosler C, Petr M, Otyepka M, et al. (2016) Biomimetic superhydrophobic/superoleophilic highly fluorinated graphene oxide and zif-8 composites for oil-water separation. Angew Chem Int Ed 55: 1178-1182.

15. Feng X, Jiang L (2006) Design and creation of superwetting/antiwetting surfaces. Adv Mater 18: 3063-3078.

16. Wang JN, Zhang YL, Liu Y, Zheng WH, Lee LP, et al. (2015) Recent developments in superhydrophobic graphene and graphene-related materials: from preparation to potential applications. Nanoscale 7: 7101-7114.

17. Drelich J, Chibowski E (2010) Superhydrophilic and superwetting surfaces: Definition and mechanisms of control. Langmuir 26: 18621–18623.

18. Hsieh CT, Yang BH, Tzou DY, Chen YF, Chen WY (2013) Liquid repellency from graphite sheets with di9erent oxidation levels. Uin Solid Films 529: 80-84.

19. Wang G, Yang J, Park J, Gou X, Wang B, et al. (2008) Facile synthesis and characterization of graphene nanosheets. J Phys Chem C 112: 8192-8195.

20. Chambers A, Park C, Terry R, Baker K, Rodriguez MN (1998) Hydrogen storage in graphite nanofibers. J Phys Chem B 102: 447-4482.

21. Chen W, Yan L (2010) Preparation of graphene by a low-temperature thermal reduction at atmosphere pressure. Nanoscale 2: 559-563.

22. Kostiuk D, Bodik M, Si9alovic P, Jergel M, Halahovets Y, et al. (2016) Reliable determination of the few-layer graphene oxide thickness using Raman spectroscopy J Raman Spectr 47: 391–394.

23. Luo ZQ, Yu T, Kim KJ, Ni ZH, You YM, et al. (2009) Uickness-dependent reversible hydrogenation of graphene layers. ACS Nano 7: 1781–1788.

24. Elias DC, Nair RR, Mohiuddin TMG, Morozov SV, Blake P, et al. (2009) Control of graphene's properties by reversible hydrogenation: Evidence for graphane. Science 323: 610–613.

25. Adamson AW (1990) Physical chemistry of surfaces (5th edn.). Wiley–Interscience, New York.

26. Moskovits M (1985) Surface-enhanced spectroscopy. Rev Mod Phys 57: 783.

27. Wenzel RN (1936) Resistance of solid surfaces to wetting by water. Ind Eng Chem 28: 988.

28. Cassie ABD, Baxter S (1944) Wettability of porous surfaces. Trans Faraday Soc 40: 546-561.

29. Quere D (2008) Wetting and Roughness. Annu Rev Mater Res 38: 71-99.

30. Hare EF, Shafrin EG, Zisman WA (1954) Properties of films of adsorbed fluorinated acids. J Phys Chem 58: 236–239.